Two-dimensional singlet oxygen imaging with its near-infrared luminescence during photosensitization

Bolin Hu,[a] Nan Zeng,[a] Zhiyi Liu,[a] Yanhong Ji,[b] Weidong Xie,[a] Qing Peng,[c] Yong Zhou,[a] Yonghong He,[a] and Hui Ma[a]
[a]Tsinghua University, Laboratory of Optical Imaging and Sensing, Graduate School at Shenzhen, Shenzhen, 518055, China
[b]China Normal University, MOE Key Laboratory of Laser Life Science & Institute of Laser Life Science, South Guangzhou 510631, China
[c]Shanghai Jiaotong University, Xinhua Hospital, School of Medicine, Department of Ophthalmology, Shanghai 200092, China

Abstract. Photodynamic therapy is a promising cancer treatment that involves activation of photosensitizer by visible light to create singlet oxygen. This highly reactive oxygen species is believed to induce cell death and tissue destruction in PDT. Our approach used a near-infrared area CCD with high quantum efficiency to detect singlet oxygen by its 1270-nm luminescence. Two-dimensional singlet oxygen images with its near-infrared luminescence during photosensitization could be obtained with a CCD integration time of 1 s, without scanning. Thus this system can produce singlet oxygen luminescence images faster and achieve more accurate measurements in comparison to raster-scanning methods. The experimental data show a linear relationship between the singlet oxygen luminescence intensity and sample concentration. This method provides a detection sensitivity of 0.0181 μg/ml (benzoporphyrin derivative monoacid ring A dissolved in ethanol) and a spatial resolution better than 50 μm. A pilot study was conducted on a total of six female Kunming mice. The results from this study demonstrate the system's potential for *in vivo* measurements. Further experiments were carried out on two tumor-bearing nude mice. Singlet oxygen luminescence images were acquired from the tumor-bearing nude mouse with intravenous injection of BPD-MA, and the experimental results showed real-time singlet oxygen signal depletion as a function of the light exposure. © *2011 Society of Photo-Optical Instrumentation Engineers (SPIE).* [DOI: 10.1117/1.3528593]

Keywords: photosensitization; singlet oxygen luminescence; two-dimensional imaging.

Paper 10357RR received Jun. 25, 2010; revised manuscript received Nov. 7, 2010; accepted for publication Nov. 9, 2010; published online Jan. 12, 2011.

1 Introduction

Photodynamic therapy (PDT) is an emerging therapy for the treatment of diseases ranging from cancer treatment to some nonmalignant conditions.[1–3] In PDT, photosensitizer (PS) incorporated into abnormal tissues is irradiated with visible light.[2,3] Photoexcited sensitizer transfers energy to the ground-state oxygen via the type-Π photochemical pathway to produce singlet oxygen ($^1O_2$).[4] Singlet oxygen is an important intermediate in many chemical and biological processes and believed to play significant roles in tumor cell death and tissue destruction during PDT.[4–6] Detection of singlet oxygen has been investigated by using electron spin resonance, fluorescence probes and chemiluminescence (CL) probes.[7–10] In comparison with those singlet oxygen detection tools, monitoring the production of singlet oxygen by measuring its luminescence at 1270 nm ($a^1\Delta_g \rightarrow X^3\Sigma_g^-$) would provide an ultimate marker and an ideal dosimetry technique.

In the past years, singlet oxygen has been directly detected by its weak 1270-nm luminescence.[11–13] Whereas the detection of singlet oxygen luminescence signal was performed on bulk samples, and the measurements were averaged over the bulk samples in many of these studies. However considering the inhomogeneities in PS distribution, oxygen concentration, and/or the space intensity of exciting light, which can affect the production and behavior of singlet oxygen, various methods have been further proposed for the measurements of spatial distribution of singlet oxygen by its luminescence at 1270 nm.[14–17] In these methods, photomultiplier tubes or linear detector arrays were used to obtain $^1O_2$ luminescence images from the 1270-nm weak emission. In 2002, Klembt *et al.* reported a singlet oxygen image with a spatial resolution of 2.5 μm detected by an InGaAs linear array.[14] In 2004, Zebger *et al.* used a linear InGaAs device to create a singlet oxygen image of a single cell.[15] In 2005, Niedre *et al.* used a laser-scanning system to image $^1O_2$ luminescence in an intradermal tumor model in mice.[16] In 2009, Breitenbach *et al.* reported singlet-oxygen-based images of a cell obtained by raster-scanned method.[17] These scanning-based researches have improved the $^1O_2$ luminescence imaging methodology and developed tools that could provide more information for basic photobiological research and PDT dosimetry.

In the scanning-based $^1O_2$ luminescence imaging methods,s a high demand for the motion precision of the moving stage as well as the edge-overlap restructuring algorithm used to remove large position errors and join traces in image reconstruction, resulting in complexity of the system and adverse effect on the measurement accuracy.[18] Moreover, because the long

Address all correspondence to: Yonghong He, Tsinghua University, Graduate School at Shenzhen, Laboratory of Optical Imaging and Sensing, Shenzhen, 518055, China. Tel: 008675526036361; Fax: 008675526036395; E-mail: heyh@sz.tsinghua.edu.cn.

integration time is needed in each scan for the weak $^1O_2$ luminescence signal and image data need to be collected sequentially, scanning image methods need a relatively long time to acquire an image. This may bring adverse influence to the final results because of the changes of parameters mentioned above that can affect the production and behavior of $^1O_2$ during the data collection, as well as the time-critical *in vivo* detection of the singlet oxygen luminescence signal.[19–21] Thus, a fast-imaging technique with a relatively large imaging area and reasonable spatial resolution suitable for clinic application is necessary. In this paper, we developed a two-dimensional $^1O_2$ luminescence imaging method without scanning by use of a high quantum efficiency, high uniformity, and low dark current infrared area CCD detector. Images of photodynamically generated singlet oxygen luminescence both *in vitro* and *in vivo* have been acquired with an integration time of 1 s by this method. PS samples with different concentrations were used to test the relationship between luminescence intensity and sample concentration. The detection sensitivity of the system has been investigated, and spatial resolution of the system has been tested by exciting light spots with dark lines of various widths. In the *in vivo* experiments, a pilot study was conducted on six Kunming mice to measure $^1O_2$ luminescence *in vivo*. Three of the mice were injected with benzoporphyrin derivative monoacid ring A (BPD-MA) subcutaneously while the other mice were injected without reagents to act as controls for this part of the study. After this initial investigation, we used the proposed method below to acquire $^1O_2$ luminescence images from two tumor-bearing nude mice. One mouse was injected with BPD-MA intravenously while the other mouse was not injected with any PS.

2 Methods and Materials

2.1 Optical Imaging System Design

The schematic diagram of our experimental system is shown in Fig. 1. The whole system includes three parts: (*i*) the semiconductor laser source for excitation, (*ii*) optical filters/near-infrared (NIR) area CCD detection system, and (*iii*) a standard frame-grabber carder NI-1427 as the data acquisition system. A semiconductor laser (Changchun New Industries Optoelectronics Technology Company, Changchun, China) with a wavelength of 690 nm and a power of 100 mw, was used as light source. The laser light was collimated and fell on a beam expander. The expanded beam was reflected, and then an aperture was used to select a spot with a suitable size for both the sample and the detect range of the system. This selected light was used to photoexcite the region of interest in the sample to produce $^1O_2$ luminescence signal. An achromatic lens was used to collect the emission from the sample, which included the $^1O_2$ luminescence signal, and other possible radiations, such as PS fluorescence, backscattered laser light, and autofluorescence from tissues *in vivo*. The emission feature of singlet oxygen was centered in the wavelength region of 1270 $\pm$ 10 nm. Spectral discrimination of the singlet oxygen emission from the interference mentioned above was achieved by using a long-pass filter (LP1150, Thor labs) and a NIR bandpass filter (1270BP20, Omega optical) centered at 1270 nm with a full width at half maximum of 20 nm and an attenuation optical density (OD) better than OD5. The transmitted emission from the filters was coupled by an
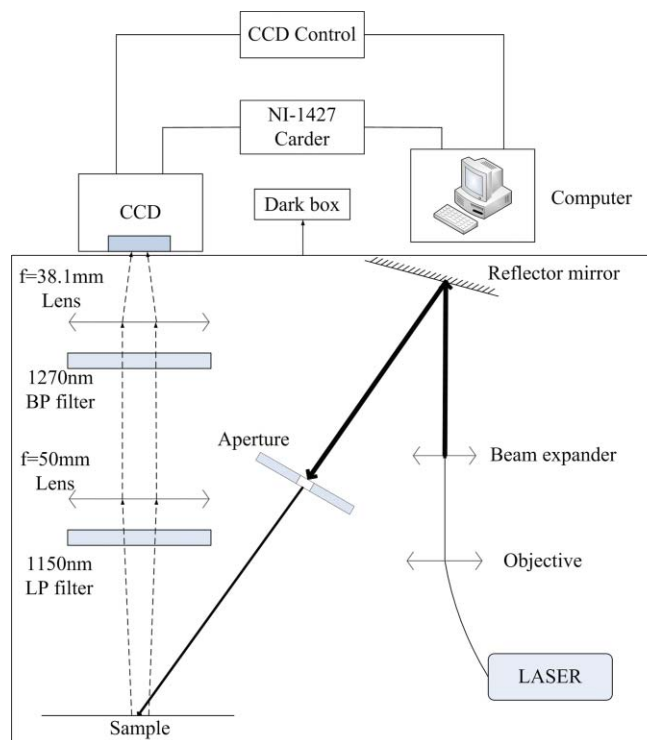

Fig. 1 Schematic layout of the NIR area CCD-based $^1O_2$ luminescence imaging system.

NIR lens onto an InGaAs area detector (XEVA-CL-FPA-1.7–320-TE1–60Hz, Xenics), whose spectra response ranged from 900 to 1700 nm with a uniform quantum efficiency of 84%. The CCD surface was cooled at –20°C to reduce thermal noise. We used a standard frame-grabber carder NI-1427 for the image data acquisition. Because of the high quantum efficiency of the NIR area CCD, it showed strong capability in weak-signal detection. Throughout our study, singlet oxygen luminescence images could be acquired with an integration time as short as 1 s. In addition, due to the area imaging method, the proposed system could achieve two-dimensional measurement of singlet oxygen without scanning. Thus, the proposed system was able to produce singlet oxygen luminescence images faster than the raster-scanning methods.

2.2 Experimental Sections

In the study, benzoporphyrin derivative monoacid ring A [(BPD-MA), Novartis Ophthalmics Europe Ltd., Basle, Switzerland] was dissolved in 75% ethanol in different concentrations and then illuminated with light source to produce $^1O_2$. BPD-MA has been studied as a PS for photodynamic therapy in age-related macular degeneration and presents a rather high singlet oxygen quantum yield in ethanol (φ_Δ = 0.81).[22] All samples were held in a 10 $\times$ 10 $\times$ 5 mm quartz cuvette mounted on a sample stage, which was able to maintain the source-sample-detector geometry constant during experiments. The space intensity of the exciting light was 60 mw/cm^2, and images were captured at an exposure time of 1 s throughout these experiments.
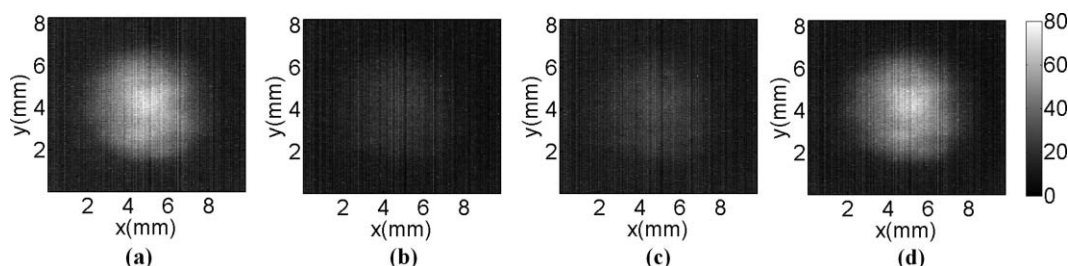
Fig. 2 Comparison of near-IR emission centered at wavelength 1270 ± 10 nm, detected from BPD-MA in ethanol: (a) sample with no additional reagents added, (b) sample with addition of singlet oxygen quencher DABCO, (c) sample deoxygenated, and (d) sample in (c) oxygenated environment.

In order to show that it was able to measure singlet oxygen luminescence by this system *in vivo*, a pilot study was conducted on a total of six female Kunming mice (Experimental Animal Centre of San Yat-sen University of Medical Science, Guangzhou, China). In this study, BPD-MA was dissolved in 5% dextrose-in-water solution, as illustrated in the product instruction. All the mice were anesthetized with a 1.4 mg/g intra-peritoneal dose of Urethane (Shanghai Beihe Chemicals Company, Shanghai, China), and then depilated on the zone of dorsal with 8% Na_2S (Guangzhou Chemical Reagent Factory, Guangzhou, China). For the first three mice, BPD-MA solution was subcutaneously injected into the hairless area with a 0.5-μg dosage for photosensitization. After a waiting period of 30 min, which allowed for the diffusion of PS in the tissues, light exposure was performed with a density of 60 mw/cm^2. The second set of mice was not injected with BPD-MA solution, but was irradiated using the same exciting light. This was the control group for this part of the study.

Further experiment has been done on tumor-bearing nude mice with BPD-MA intravenously injected. Two male nude mice (BALB/C, Shanghai Laboratory Animal Center, CAS, Guangzhou, China) were used to establish transplanted cancer. Tumors were induced by subcutaneous injection of a suspension of 10^6 HCT116 cells into the dorsal of seven-week-old male nude mice of 24 g weight. When the volume of the tumor reached ~120 mm^3, one of the mice received an intravenous injection of BPD-MA. After a waiting period of 3 h that allowed for the accumulation of PS in the tumor, light irradiation was performed in the anesthetized animals. Treatment irradiation of the tumor was performed with a spatial intensity of 60 mw/cm^2. The second mouse was not injected with BPD-MA, and the tumor was irradiated by the same exciting light as in the control group.

3 Results and Discussions

3.1 Validation of Singlet Oxygen Luminescence Signal

To demonstrate that the signal detected by our system was indeed derived from singlet oxygen, experiments were performed with three samples of BPD-MA dissolved in 75% ethanol at the concentration of 0.5 μg/ml. The first sample contained no additional reagents, whereas the second sample had 1,4-Diazabicyclo[2,2,2]octane [(DABCO), Guangzhou Aladdin Reagent Company, Guangzhou, China], an acknowledged quencher of singlet oxygen, added to it. The last one was first

bubbled with nitrogen gas to displace the dissolved oxygen, and then the bubbling stopped and the sample was exposed to air. Figure 2 shows the singlet oxygen images of samples irradiated by the exciting light of the same fluence rate. In Fig. 2(a), the shapes and details of the $^1O_2$ luminescence image were observed from the sample with no additional reagents added. As expected, in Fig. 2(b) the NIR signal disappeared with the addition of DABCO. Similarly, the signal was absent from the
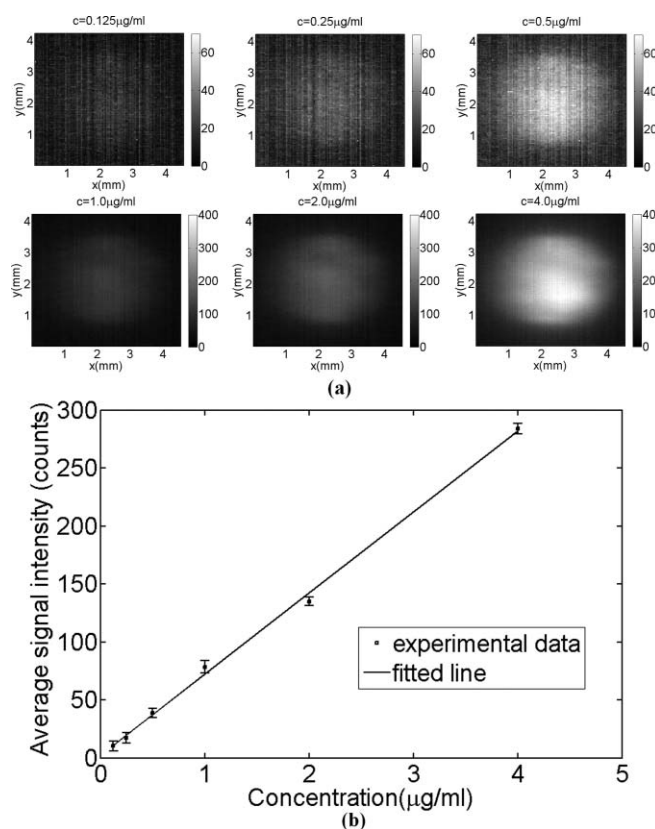
Fig. 3 Detection of singlet oxygen luminescence from BPD-MA samples with different concentrations. (a) Images of BPD-MA dissolved in 75% ethanol with the concentration of 0.125, 0.25, 0.5, 1.0, 2.0, and 4.0 μg/ml from the top left to bottom right. The top images use colorbar ranging from 0 to 70 and the bottom images have a color bar ranging from 0 to 400. (b) The dependence of average $^1O_2$ signal intensity on the concentration of BPD-MA samples derived from (a), the linear fitting give an r^2 value of 0.993, and the error bars represent the standard deviation of three samples with the same concentration in each concentration.
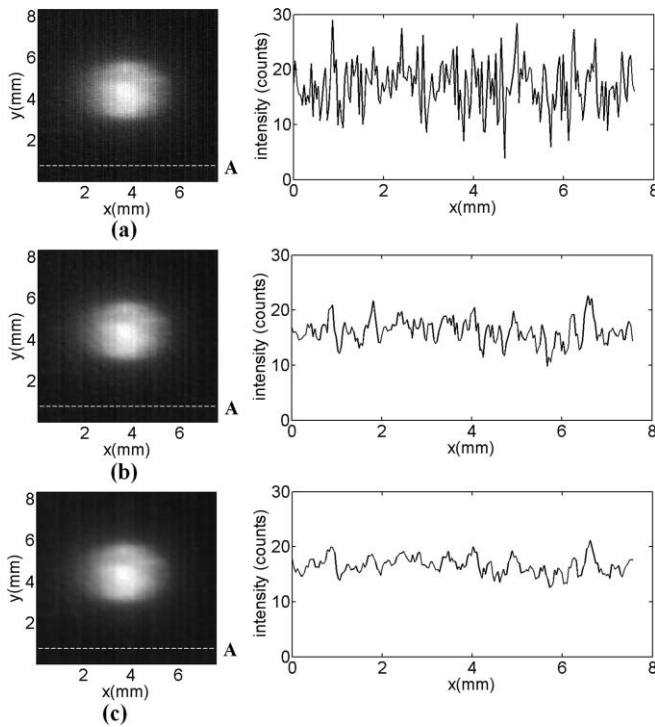
Fig. 4 Effects of spectral smoothing, linear spatial filter used for reducing noise level. (a) original singlet oxygen luminescence image, (b) 3 × 3 pixels, (c) 5 × 5 pixels neighborhood are averaged to replace each pixel. Intensity graphs of dashed row A, across the background, are plotted on the right side of these images. The SNRs achieved from (a), (b), and (c) are 20.0621, 37.7165, and 55.2642, respectively.

sample equilibrated with nitrogen, as shown in Fig. 2(c). When nitrogen bubbling stopped and the sample equilibrated with nitrogen previously was exposed to air, the signal appeared again due to the diffusion of air back into the liquid sample, as shown in Fig. 2(d).

3.2 *Linear Sensing Range and Detection Sensitivity*

BPD-MA was dissolved in 75% ethanol with concentrations of 0.125, 0.25, 0.5, 1.0, 2.0, and 4.0 μg/ml. These samples were prepared in order to test the linear sensing range of the system. A background image was recorded after the irradiation of 75% ethanol without PS dissolved. The $^1O_2$ luminescence images were taken immediately after the start of the irradiation. In this series, each pixel represents the background-subtracted signal at 1270 nm. Figure 3(a) shows the series of $^1O_2$ lumines-

cence images of samples with different concentrations. It is clear that the $^1O_2$ luminescence signal increases with the increasing of sample density for the same fluence rate. From the data in Fig. 3(a), the average $^1O_2$ luminescence intensities are 10.3, 17.2, 38.9, 78.4, 134.9, and 283.9 counts, respectively, as plotted in Fig. 3(b). These average signal intensities were calculated by integration method, which averaged data between upper and lower limits in the image. The upper limit, which was used to remove the hot pixels in the spectral image, was determined by the mean of pixel value in region of signal area, and the lower limit was determined by the mean of background in the image and the mean of pixel value in region of signal area. The relationship between the average $^1O_2$ luminescence intensity and the concentration of the BPD-MA is shown in Fig. 3(b). It was found that the average $^1O_2$ luminescence intensity showed a linear relationship with the concentration of BPD-MA from 0.125 to 4 μg/ml. The linear fitting analysis gave an r^2 of 0.993.

We could calculate the detection sensitivity of the system as follos:[23,24]

$$S_d = D_s/\text{SNR} \tag{1}$$
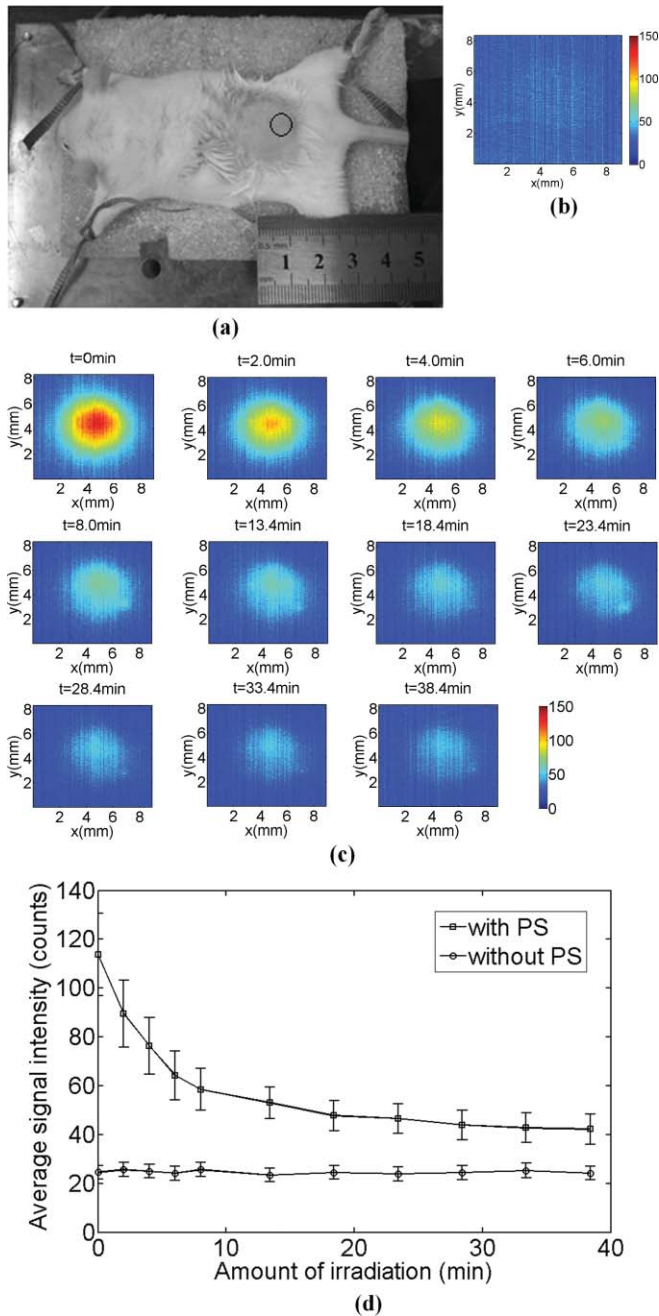
where S_d is the detection sensitivity, D_s, the sample density, and SNR is the signal-to-noise ratio. In this study, we used the 1.0 μg/ml BPD-MA solution to test the detection sensitivity and $^1O_2$ luminescence image was acquired immediately after the start of the irradiation. Figure 4(a) is the original image acquired by our system and the intensity graph of marked row A. In Figs. 4(b) and 4(c), the value of every pixel was replaced by the average of the intensity levels in the 3 × 3 and 5 × 5 neighborhood, as a smoothing, linear spatial filter to further enhance the SNR. The definition of SNR is the ratio of signal intensity to the standard deviation of background. In Fig. 4, the average singlet oxygen signal intensity is 89.0 counts and the standard deviations of the background are 4.4579, 2.3623, and 1.6096, respectively. Thus, the SNR achieved from Fig. 4 was 20.0621, 37.7165, and 55.2642, respectively. According to Eq. (1), as the sample density D_s is 1.0 μg/ml, the sensitivity of our system can achieve 0.0181 μg/ml with a SNR of 55.2642 as a result of a 5 × 5 smoothing, linear spatial filter. The cost of smoothing, linear spatial filter is the reduction of spatial resolution.

3.3 *Resolving Power*

The pixel size of the area CCD is 30 × 30 μm, and the magnification of this system is 0.762. The spatial resolution of 39.4 μm can be calculated in theory. To investigate the spatial resolution of the system, a series of filaments with diameters (*D*) of 200, 150, 100, and 50 μm were set in the center of the cross section
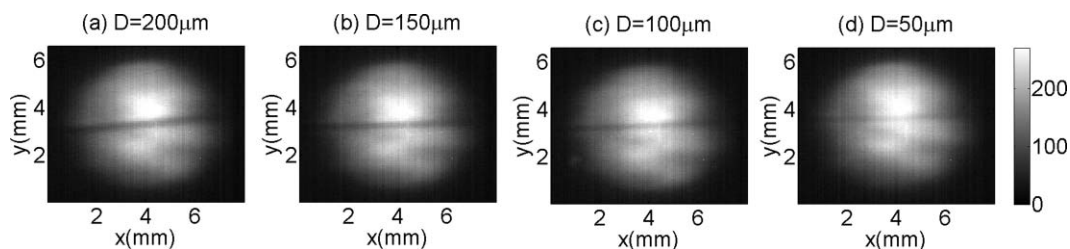
Fig. 5 The spatial resolution of the system: The $^1O_2$ luminescence images of BPD-MA samples excited by the divided laser lights with dark lines of (a) 200, (b) 150, (c) 100, and (d) 50 μm widths, respectively. All the images were obtained with an integration time of 1 s.

(a)

(b)

t=0min t=2.0min t=4.0min t=6.0min

t=8.0min t=13.4min t=18.4min t=23.4min

t=28.4min t=33.4min t=38.4min

(c)

(d)

Fig. 6 (a) White-light image of a Kunming mouse, the area marked by a circle is for irradiation. (b) 1270-nm emission detection from one of the mice without BPD-MA injected during irradiation. (c) Singlet oxygen luminescence time series-image obtained from one of the mice injected with BPD-MA subcutaneously during light exposure. (d) The dependence of average light intensity on the amount of irradiation, each point represents the mean of the average spatial light intensities obtained from three animals. The error bars represent the standard deviation between the three animals in each experiment. The singlet oxygen images in (b) and (c) were acquired with an integration time of 1 s.

of the collimated laser beam, sequentially. Thus, the exciting light was divided to form a light spot with a dark line in the center. Figure 5 shows the $^1O_2$ luminescence images obtained on irradiation of BPD-MA dissolved in 75% ethanol. The dark fringe appeared in each of the images in Fig. 5, and each one could be distinguished. However the sharpness of dark fringes

in the images deteriorated with the reduction of the dark line's width in the laser light. Because the dark fringe in the last image can be distinguished, corresponding to the 50-μm case; thus, the spatial resolution of the system is <50 μm. The resolving power, which could further be optimized by improving the magnification of the system, is sufficient and has promise in singlet oxygen monitoring in PDT.

3.4 Singlet Oxygen Luminescence Imaging In Vivo

A pilot study was conducted on a total of six female Kunming mice to demonstrate the system's potential *in vivo*. One group of three mice was injected with BPD-MA subcutaneously at 0.5 μg dosage, and the other group of three mice was injected without BPD-MA. Figure 6 shows the results of the pilot experiments *in vivo*. Figure 6(a) is a white-light image of a Kunming mouse taken using a commercial digital camera (Olympus, E300). The area marked by a circle represents the tissue area irradiated by the laser. Figure 6(b) illustrates singlet oxygen images obtained from one of the Kunming mice without subcutaneous injection of BPD-MA during irradiation. The CCD integration time was 1 s. This image was not background corrected, thus representing the background emission. Figure 6(c) shows a $^1O_2$ luminescence image series acquired from one of the mice with subcutaneous injection of BPD-MA. Each image was obtained with an integration time of 1 s. These images illustrated the singlet oxygen luminescence from the area irradiated during light exposure. Compared to the weak light acquired from the mouse without PS, shown in Fig. 6(b), the $^1O_2$ luminescence could be measured clearly from the mouse injected with PS *in vivo*, as shown in Fig. 6(c). From the data obtained from the two groups, the average $^1O_2$ luminescence signal intensity as a function of the amount of irradiation can be calculated by the integration method, as shown in Fig. 6(d). The curve that represents signal change from Kunming mice with subcutaneous injection of BPD-MA shows a decreasing $^1O_2$ luminescence signal during the long exposure time, compared to the weak light intensity and no intensity depletion in the case without BPD-MA. Because this data set was not background subtracted, the data mainly represent the background light present in the measurements. The causes for the reduction in $^1O_2$ signal might likely be due to PS photobleaching, the photochemical depletion of molecular oxygen in tissues.[25,26] The error bars in Fig. 6(d) represent the standard deviation between the three animals in each experiment.

Because the use of tumor-bearing model to study PS accumulation and reactive oxygen species (ROS) production under laser irradiation has high relevance and intravenous injection can be an accurate method of efficient tissue diffusion, we used two tumor-bearing nude mice for further experiments. One of the mice was infused with a BPD-MA concentration of 1.50 mg/kg body weight, as per product instructions. The other mouse in the study was not injected with BPD-MA. Figure 7(a) is a white-light image of a tumor-bearing nude mouse with the tumor area irradiated with the laser marked by a circle. Figure 7(b) shows the NIR emission from the tumor-bearing mice without intravenous injection of BPD-MA at the moment when the amount of irradiation was 15 s. The CCD integration time was 1 s. Similar to Fig. 6(b), Fig. 7(b) represents the background emission too. Figure 7(c) shows an $^1O_2$ luminescence image series acquired from the tumor-bearing mouse with intravenous injection of
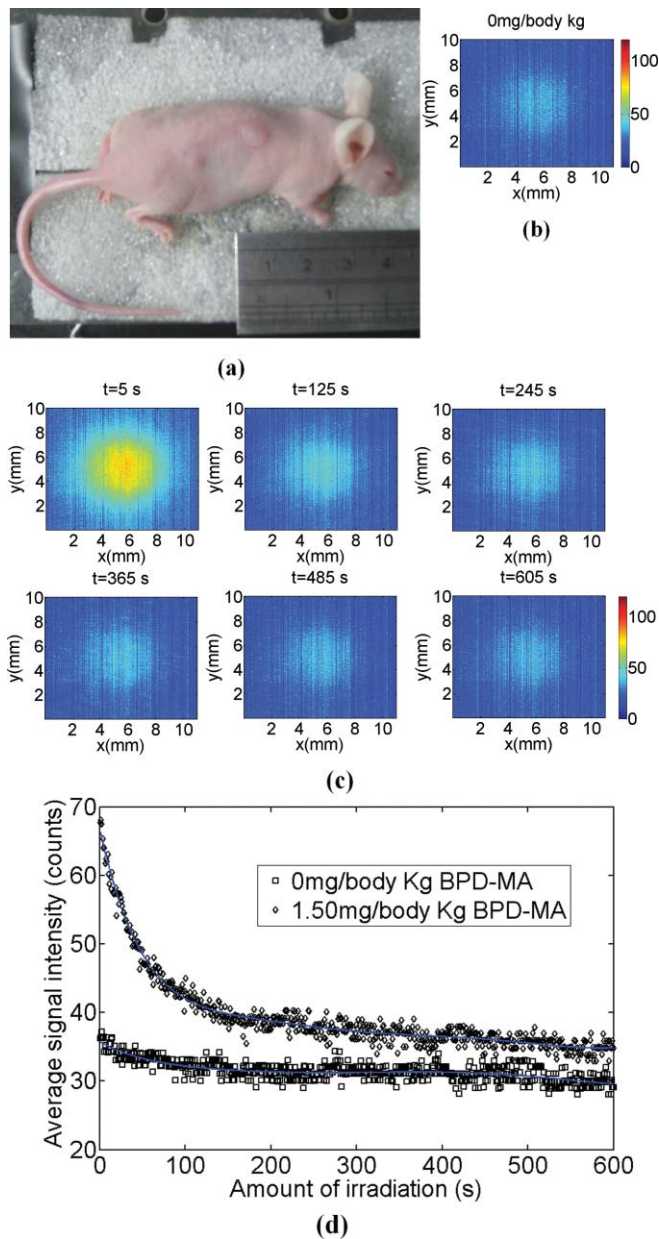
Fig. 7 (a) White-light image of a tumor-bearing nude mouse; the tumor for irradiation is marked by a circle. (b) The measurement of singlet oxygen from the tumor in the mouse without intravenous injection of BPD-MA during irradiation. (c) Singlet oxygen luminescence time series-image obtained from the tumor in the mouse injected with BPD-MA intravenously during light exposure. (d) Real-time average singlet oxygen signal depletion as a function of the light exposure. The singlet oxygen luminescence images in (b) and (c) were acquired with an integration time of 1 s.

BPD-MA. Each image was obtained with an integration time of 1 s. These images represent measurements of singlet oxygen in the tumor tissues during PDT. We recorded singlet oxygen luminescence images from both the tumor-bearing nude mice to monitor the singlet oxygen changes during long-term light exposure. All images were recorded with an integration time of 1 s. Average singlet oxygen signal intensity was calculated from these images by integration method. Figure 7(d) shows average singlet oxygen signal intensity's depletion in real time

as a function of the amount of irradiation and presents data for 600 s of light exposure. Data analysis of these measurements was performed without any background subtraction. By analyzing the spectral images from Figs. 6(d) and 7(d), the signal intensity from the mice injected with BPD-MA (both subcutaneously and intravenously) was obviously stronger than the signal from the mice without injection of BPD-MA. The signal shows similar depletion trend from both Kunming mouse with subcutaneous injection of BPD-MA and tumor-bearing nude mouse with intravenous injection of BPD-MA, indicating that the singlet oxygen measurement could be achieved *in vivo* during PDT by this proposed system.

4 Conclusions

We have introduced a new NIR area CCD-based $^1O_2$ luminescence two-dimensional imaging method for photosensitization and successfully applied this system to detecting singlet oxygen by its 1270-nm emission during photosensitization both *in vitro* and *in vivo*. The experimental system has a detection sensitivity of 0.0181 μg/ml (BPD-MA dissolved in 75% ethanol) and a resolving power of <50 μm. We obtained photodynamically generated $^1O_2$ luminescence images from Kunming female mice injected with BPD-MA subcutaneously. Further experiments have been conducted on tumor-bearing nude mice with intravenous injection of BPD-MA. Measurement of singlet oxygen distribution was achieved from the tumor area, and singlet oxygen signal depletion in real-time as a function of the light exposure was observed. Using this method, we demonstrated that $^1O_2$ luminescence images could be acquired with an integration time of 1 s both *in vitro* and *in vivo*, without scanning. Because short CCD capture times and two-dimensional imaging were used, the system could produce singlet oxygen luminescence images faster and achieve more accurate measurements. We believe that the proposed NIR area CCD-based $^1O_2$ luminescence two-dimensional imaging method is promising for *in vivo* monitoring of singlet oxygen produced during PDT.

References

1. T. J. Dougherty, C. J. Gomer, B. W. Henderson, G. Jori, D. Kessel, M. Korbelik, J. Moan, and Q. Peng, "Photodynamic therapy," *J. Natl Cancer Inst.* **90**, 889–905 (1998).
2. B. C. Wilson and M. S. Patterson, "The physics, biophysics and technology of photodynamic therapy," *Phys. Med. Biol.* **53**, R61–R109 (2008).
3. M. Panjehpour, B. F. Overholt, M. N. Phan, and J. M. Haydek, "Optimization of light dosimetry for photodynamic therapy of Barrett's esophagus: efficacy vs. incidence of stricture after treatment," *Gastrointest. Endosc.* **61**, 13–18 (2005).
4. C. Schweitzer and R. Schmidt, "Physical mechanisms of generation and deactivation of singlet oxygen," *Chem. Rev.* **103**, 1685–1757 (2003).
5. B. H. Li, M. T. Jarvi, E. H. Moriyama, and B. C. Wilson, "Correlation between cell viability and cumulative singlet oxygen luminescence from protoporphyrin IX in varying subcellular localizations," *Proc. SPIE.* **6427**, 1–7 (2007).

6. D. Kessel and Y. Luo, "Mitochondrial photodamage and PDT-induced apoptosis," *J. Photochem. Photobiol. B.* **42**, 89–95 (1998).

7. Y. Lion, M. Delmell, and A. Van de Vorst, "New method of detecting singlet oxygen production," *Nature* **263**, 442–443 (1976).

8. M. M. Tarpey and I. Fridovich, "Methods of detection of vascular reactive species nitric oxide, superoxide, hydrogen peroxide, and peroxynitrite," *Circ. Res.* **89**, 224–236 (2001).

9. R. P. Rastogi, S. P. Singh, D. Häder, and R. P. Sinha, "Detection of reactive oxygen species (ROS) by the oxidant-sensing probe $2',7'$-dichlorodihydrofluorescein diacetate in the cyanobacterium Anabaena variabilis PCC 7937," *Biochem. Biophys. Res. Commun.* **397**, 603–607 (2010).

10. S. Yamaguchi, N. Kishikawa, K. Ohyama, Y. Ohba, M. Kohno T. Masuda, A. Takadate, K. Nakashima, and N. Kuroda, "Evaluation of chemiluminescence reagents for selective detection of reactive oxygen species," *Anal. Chim. Acta.* **665**, 74–78 (2010).

11. A. A. Krasnovsky, "Singlet molecular oxygen in photobiochemical systems: IR phosphorescence studies," *Membr. Cell Biol.* **12**, 665–690 (1998).

12. M. J. Niedre, C. S. Yu, M. S. Patterson, and B. C. Wilson, "Singlet oxygen luminescence as an in vivo photodynamic therapy dose metric: validation in normal mouse skin with topical amino-levulinic acid," *Br. J. Cancer.* **92**, 298–304 (2005).

13. S. Lee, D. H. Vu, S. J. Davis, A. Liang, and T. Hasan, "Pulsed diode laser-based singlet oxygen monitor for photodynamic therapy: *in vivo* studies of tumor-laden rats," *J. Biomed. Opt.* **13**, 064035 (2008).

14. L. K. Andersen, Z. Gao, P. R. Ogilby, L. Poulsen, and I. Zebger, "A Singlet oxygen image with 2.5 μm resolution," *J. Phys. Chem. A* **106**, 8488–8490 (2002).

15. I. Zebger, J. W. Snyder, L. K. Andersen, L. Poulsen, and Z. Gao, "Direct optical detection of singlet oxygen from a single cell," *Photochem. Photobiol.* **79**, 319–322 (2004).

16. M. J. Niedre, M. S. Patterson, A. Giles, and B. C. Wilson, "Imaging of photodynamically generated singlet oxygen luminescence *in vivo*," *Photochem. Photobiol*. **81**, 941–943 (2005).

17. T. Breitenbach, M. K. Kuimova, P. Gbur, S. Hatz, N. B. Schack, B. W. Pedersen, J. D. C. Lambert, L. Poulsen, and P. R. Ogilby, "Photosensitized production of singlet oxygen: spatially-resolved optical studies in single cells," *Photochem. Photobiol. Sci.* **8**, 442–452 (2009).

18. G. L. Huang, C. Deng, J. Zhu, S. K. Xu, C. Han, X. B. Song, and X. Y. Yang, "Digital imaging scanning system and biomedical applications for biochips," *J. Biomed. Opt.* **13**, 034006 (2008).

19. S. Iinuma, K.T. Schomacker, G. Wagnieres, M. Rajadhyaksha, M. Bamberg, and T. Momma, "*In vivo* fluence rate and fractionation effects on tumor response and photobleaching: photodynamic therapy with two photosensitizers in an orthotopic rat tumor model," *Cancer Res.* **59**, 6164–6170 (1999).

20. J. Baier, T. Maisch, J. Regensburger, M. Loibl, R. Vasold, and W. Bäumler, "Time dependence of singlet oxygen luminescence provides an indication of oxygen concentration during oxygen consumption," *J. Biomed. Opt.* **12**, 064008 (2007).

21. J. W. Snyder, E. Skovsen, J. D.C. Lambert, L. Poulsen, and P. R. Ogilby, "Optical detection of singlet oxygen from single cells," *Phys. Chem. Chem. Phys.* **8**, 4280–4293 (2006).

22. H. Christophe, W. Georges, M. Philippe, and B. Hubert, "EPR and spectrophotometric studies of free radicals (O_2^-, OH, BPD-MA$^-$) and singlet oxygen ($^1O_2$) generated by irradiation of benzoporphyrin derivative monoacid ring A," *Photochem. Photobiol.* **65**, 818–827 (1997).

23. C. Nicolini, A. M. Malvezzi, A. Tomaselli, D. Sposito, G. Tropiano, and E. Borgogno, "DNAS I: layout and data analysis," *IEEE Trans Nanobiosci.* **1**, 67–72 (2002).

24. R. Nagarajan and C. A. Peterson, "Identifying spots in microarray images," *IEEE Trans. Nanobiosci.* **1**, 78–84 (2002).

25. V. H. Fingar, T. J. Wieman, S. A. Wiehle, and P. B. Cerrito, "The role of microvascular damage in photodynamic therapy: the effect of treatment on vessel constriction, permeability, and leukocyte adhesion," *Cancer Res.* **52**, 4914–4921 (1992).

26. B. W. Henderson, T. M. Busch, L. A. Vaughan, N. P. Frawley, D. Babich, T. A. Sosa, J. D. Zollo, A. S. Dee, M. T. Cooper, D. A. Bellnier, W. R. Greco, and A. R. Oseroff, "Photofrin photodynamic therapy can significantly deplete or preserve oxygenation in human basal cell carcinomas during treatment, depending on fluence rate," *Cancer Res*. **60**, 525–529 (2000).